Reduction of the Grating Lobes of Annular Arrays Used in Focused Ultrasound Surgery

Florence Dupenloup, Jean Yves Chapelon, *Member, IEEE,* Dominique J. Cathignol, *Member, IEEE,* and Oleg A. Sapozhnikov

Abstract— **An annular array with variable focus, used in focused ultrasound surgery, generates grating lobes responsible for undesirable lesions. It is known that the amplitude and the location of the lobes depend on both the geometry and the frequency of the transducer. A new procedure based on the use of a wide-band CW signal, i.e., a signal phase modulated by a pseudorandom code, is proposed to reduce the amplitude of these lobes. The theoretical study enables us to determine the location and the amplitude of these lobes and to simulate the effect of the transmitted signal bandwidth. In particular, a simple analytical relation gives the intensity ratio between the grating lobes and the main lobe. This equation shows that this ratio is inversely proportional to the number of rings and to the bandwidth of the transmitted signal. A system was developed and tested with two transducer arrays of 35- and 150-mm diameter, respectively. The simulations and experiments demonstrate the validity of the theoretical study and the efficacy of the proposed procedure. In conclusion, it is possible to reduce the grating lobes without geometric modification of the array by increasing the bandwidth of the transmitted signal.**

I. Introduction

THE USE OF high-intensity focused ultrasound (HIFU) for noninvasive local ablation of precisely defined target volume within tissue seems originally to have been formulated by Fry [1]. It is only recently, however, that new clinical applications, including some in cancer therapy, have been developed [2]–[4]. This technique of therapy using HIFU is also known as focused ultrasound surgery. The ultrasound intensity generated by a highly focused transducer increases from the source to the focus where it reaches a very high level. The absorption of the ultrasonic energy at the focus induces a sudden temperature rise which causes the irreversible ablation of the targeted cells without damaging the intermediate tissues. The destroyed zone, defined as an elementary lesion, has a volume of a few cubic millimeters, slightly in front of the geometric focus.

To treat a large volume, it is necessary to reproduce this elementary lesion by displacing the focal point of the transducer. Up to now, this displacement has been performed mechanically. Recently, studies based on the principle of the ultrasound scanner have shown the feasibility [5] of using dynamic focusing in ultrasonic therapy. In this method the focal point is displaced electronically, offering the advantage of being less costly and more accurate. The main drawback of this procedure is the generation of secondary lobes, called grating lobes, by a single frequency CW signal. The intensity of these lobes, which can be greater than that of the main lobe, may be responsible for undesirable tissue necroses located outside the target volume. This problem has been solved in ultrasound hyperthermia by apodizing the energy on each ring of the array in order to ensure a homogenous ultrasonic field [6], [7]. Unfortunately, in this case the power applied on the transducer array is not uniform and local overstepping of the cavitation threshold may result, which is recognized as a limit of the technique [8].

It is known that the location and amplitude of these lobes depend directly on the transducer geometry and the frequency of the ultrasonic waves. The larger the number of rings, the lower the amplitude of the grating lobes. However, this solution increases the complexity and the cost of the electronic channels. It is therefore advantageous to define the transducer geometry by keeping the number of rings to a minimum. In this paper, we propose a method for reducing these lobes by using a wide-band frequency CW signal such as a pseudorandom coded signal. The advantages of a wide-band signal have already been demonstrated in different applications, such as radar [9] or imaging [10]. Here, the method is proposed for the first time in ultrasound therapy.

In the first section of this paper, a theoretical approach is presented in order to explain the effects of a wide-band signal on the grating lobes. In a parabolic approximation, this study proposes different expressions permitting the grating lobes to be characterized and the intensity ratio between the grating lobes and the main lobe to be defined. The relations obtained enable us to understand how a wide-band signal acts on the amplitude and location of the grating lobes. The second section describes the experimental system. In order to validate this study, two transducers were developed: the first one is a six-ring annular array transducer focused at 35 mm, used for the treatment of localized prostate cancer [11] and the second one is an eight-ring annular array transducer focused at 15 cm used for deeper treatments [12]. In the last section, different theoretical and experimental results are discussed.

II. Theory

This section is divided into two parts. The first part shows how the number of rings influences the acoustic pressure, and the second part gives a relation between the grating lobe intensity and the bandwidth of the signal. To simplify the

Manuscript received September 6, 1995; revised April 6, 1996.

The authors are with Unité 281, Institut National de la Santé et de la Recherche Médicale, 69424 Lyon, Cedex 03, France.

Publisher Item Identifier S 0885-3010(96)07852-5.

theoretical approach, only the pressure on the acoustic axis of the transducer is considered.

A. Effects of the Number of Transducer Rings

The annular array is composed of N rings. The space ε between each ring is constant. The rings are of equal area and so each of them generates the same acoustic power. The transducers are excited by a single frequency CW signal of frequency ν_0. The objective of this first part is to find an analytical expression of the pressure field on the acoustic axis as a function of N.

1) Study of the Pressure $p(z,t)$ Given for an Annular Array: Let us assume the transducer aperture angle θ to be sufficiently small ($\theta < 30°$). The pressure $p(z,t)$ on the acoustic axis generated by a spherical shell, in O'Neil's approximations [13], is

$$\frac{p(z,t)}{\rho c U_0} = \frac{1}{1-\frac{z}{z_0}} \times \sin 2\pi\nu_0\left(\tau - \frac{a^2}{2c}\left(\frac{1}{z}-\frac{1}{z_0}\right)\right) \quad \text{where } \tau = t - \tfrac{z}{c} \quad (1)$$

where ρ [kg/m^3] and c [m/s] are the density of the medium and the velocity of sound in the medium, a [m] and z_0 [m], respectively, are the radius and the curvature radius of the transducer (geometric focal length), z [m] is the position on the acoustic axis measured from the transducer surface, ν_0 [Hz] is the frequency of the transmitted signal, and U_0 [m/s] is the amplitude of the particle velocity that is constant over the entire surface of the transducer.

The pressure generated by each ring is the difference between the pressures created by two spherical shells whose diameters are equal to the inner and outer diameters, respectively, of the given ring. The pressure at the variable focus z_d generated by an annular array of N transducers is the sum of the pressures delivered by each ring. The delay τ_n applied to the rings is calculated from the distance between the variable focus and the center of the rings

$$\frac{p(z,\tau)}{\rho c U_0} = \sum_{n=1}^{N} \frac{p_n(z,\tau-\tau_n)}{\rho c U_0} \quad (2)$$

where $p_n(z,\tau) = p_{\text{outer transducer}}(z,\tau) - p_{\text{inner transducer}}(z,\tau)$, $\tau_n = -(n-1)a_n^2/2c(1/z_d - 1/z_0)$ with a_n the outer transducer radius of the nth ring. By considering therefore the interspace ε between each element small compared with a_n, $a_n^2 = n \times a_1^2$.

Then, (2) becomes

$$\frac{p(z,\tau)}{\rho c U_0} = \frac{1}{1-\frac{z}{z_0}} \times \sum_{n=1}^{N}\left\{\sin 2\pi\nu_0\left(\tau-\tau_n-\frac{a_n^2}{2c}\left(\frac{1}{z}-\frac{1}{z_0}\right)\right) - \sin 2\pi\nu_0\left(\tau-\tau_n-\frac{a_{n-1}^2}{2c}\left(\frac{1}{z}-\frac{1}{z_0}\right)\right)\right\}. \quad (3)$$

By using a complex notation and after some simplification, an expression of the on-axis pressure produced by an N-ring array focused at z_d is

$$\frac{p(z,t)}{\rho c U_0} = \frac{2\sin\pi\nu_0(\tau_1+\tau_2)}{1-\frac{z}{z_0}} \times \frac{\sin\pi\nu_0 N\tau_1}{\sin\pi\nu_0\tau_1} \times \cos\pi\nu_0(2\tau-\tau_2-N\tau_1) \quad (4)$$

with

$$\tau_1 = \frac{a_1^2}{2c}\left(\frac{1}{z}-\frac{1}{z_d}\right)$$

and

$$\tau_2 = \frac{a_1^2}{2c}\left(\frac{1}{z_d}-\frac{1}{z_0}\right).$$

Equation (4) highlights the influence of the different parameters. The pressure amplitude is composed of two terms: $A_1 = 2\sin\pi\nu_0(\tau_1+\tau_2)/1 - z/z_0$ which is only a characteristic of the transducer geometry and $A_2 = \sin\pi\nu_0 N\tau_1/\sin\pi\nu_0\tau_1$ which shows the effect of the dynamic focusing and of the rings, namely the grating lobes. Both coefficients A_1 and A_2 are plotted in Fig. 1. It shows that the lobes (main lobe and grating lobes) are represented by A_2. Each lobe has the same amplitude N. This result is obtained from the transducer $T1$ described in Table I.

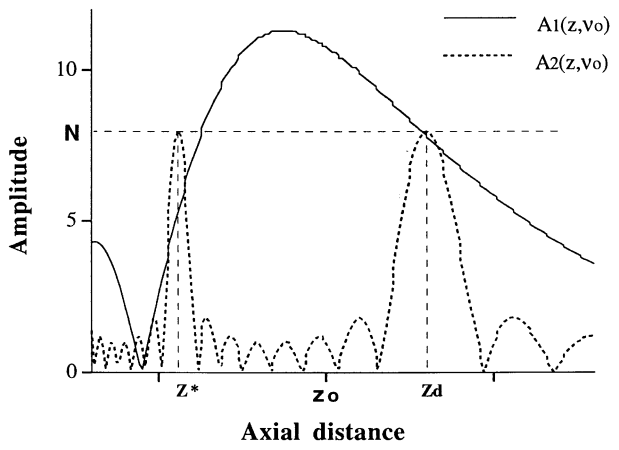

Fig. 1. Amplitude of both terms $A1$ and $A2$ of (4) as a function of the position on the acoustic axis.

2) Study of the Grating Lobes of an Annular Array: $A_2(z,\nu)$ is maximum at the given dynamic focus z_d and at the positions z^* of the grating lobes, i.e., for

$$2\pi\nu_0\tau_1 = k\pi \quad (k \in Z^*).$$

The solution of this equation is then

$$z^* = \frac{z_d}{1+kz_d\frac{2c}{a_1^2\nu_0}} \quad \text{with} \quad \begin{cases} k>0 & \text{if } z_d > z_0 \\ k<0 & \text{if } z_d < z_0. \end{cases} \quad (5)$$

The amplitude of the pressure at this point is given by

$$\left|A_1(z^*,\nu_0) \times A_2(z^*,\nu_0)\right|. \quad (6)$$

Relations (5) and (6) confirm that the location and the amplitude of the grating lobes depend on the geometry of the transducer and on the frequency of the transmitted signal. Equation (5) quickly gives the position of the grating lobes on the acoustic axis.

TABLE I
CHARACTERISTICS OF TRANSDUCERS $T1$ AND $T2$

Transducer	Frequency	Bandwidth	Diameter	Focal	Rings number	Rings area	Rings spacing
T1	2.25 MHz	1.2 MHz	35 mm	35 mm	6	19 cm^2	0.1 mm
T2	1.1 MHz	0.5 MHz	150 mm	150 mm	8	353 cm^2	0.3 mm

B. Effect of the Use of a Wide-Band Signal

The objective here is to give a relation between the acoustic intensity of the grating lobes and the signal bandwidth. For this purpose, we base our analysis on the spatial peak time average intensity (I_{SPTA}) because it is characteristic of the energy necessary to induce an elementary lesion.

The I_{SPTA} will be determined at z^*, the position of the first $(k = 1)$ grating lobes, which is the most important and at the position of the main lobe z_d. To compare the amplitude of these lobes, we express the ratio R between the intensities (I_{SPTA}) at z^* and z_d.

Using (3), an expression of the pressure may be obtained in a general case of any transmitted signal $s(t)$. Following this consideration, (3) can be rewritten as

$$p(z,\tau)=\frac{1}{1-\frac{z}{z_0}}\sum_{n=1}^{N}\{s(\tau-2(n-1)\tau_1)-s(\tau-2n\tau_1-2\tau_2)\}. \tag{7}$$

The correlation function $C_{\mathrm{pp}}(z,t)$ of the pressure $p(z,t)$ is thus written as

$$C_{\mathrm{pp}}(z,\tau) = \frac{1}{\left(1-\frac{z}{z_0}\right)^2}\sum_n\sum_k \times \begin{Bmatrix} 2C_{\mathrm{ss}}(\tau+(n-k)\tau_1) \\ -C_{\mathrm{ss}}(\tau+(n-k)\tau_1-\tau_2)-C_{\mathrm{ss}}(\tau+(n-k)\tau_1+\tau_2) \end{Bmatrix} \tag{8}$$

where $C_{\mathrm{ss}}(t)$ is the correlation function of the signal $s(t)$.

By using Fourier's transform of the correlation function $C_{\mathrm{pp}}(z,t)$, we obtain the spectral density $\phi_p(z,\nu)$ of the pressure on the acoustic axis

$$\phi_p(z,\nu)=A_1^2(z,\nu)\times A_2^2(z,\nu)\times\phi_s(\nu) \tag{9}$$

with $\phi_s(\nu)$ the spectral density of $s(t)$ and

$$A_1(z,\nu)=\frac{2\sin\pi\nu(\tau_1+\tau_2)}{1-z/z_0},\quad A_2(z,\nu)=\frac{\sin\pi\nu N\tau_1}{\sin\pi\nu\tau_1}.$$

The ratio R is written

$$R=\int_{-\infty}^{+\infty}\phi_p(z^*,\nu)d\nu\Big/\int_{-\infty}^{+\infty}\phi_p(z_d,\nu)d\nu. \tag{10}$$

When the transmitted signal is a sine wave of frequency ν_0, its spectral density is a Dirac function, and in this case $A_2^2(z^*,\nu_0)=A_2^2(z_d,\nu_0)=N^2$. The ratio R, noted in this case as R_0, then becomes

$$R_0=A_1^2(z^*,\nu_0)/A_1^2(z_d,\nu_0). \tag{11}$$

For a transmitted signal of a bandwidth B, (10) becomes very complex. To obtain an analytical expression of the ratio R, a number of approximations are necessary.

1) The spectral density $\phi_s(z,\nu)$ of $s(t)$ is approximated by a Gaussian function of bandwidth B, i.e., $\phi_s(\nu)=B\times e^{-(\nu-\nu_0/B)^2}$. This approximation may be justified in most cases considering that the shape of $\phi_s(\nu)$ is given by the impulse response of the transducer.
2) The locations of the grating lobes versus the frequency ν $(\nu\in B)$ being small: $1/z-1/z^*\ll 1$ where $z^*=z^*(\nu_0)$ is given by (5) and $z=z_d/1\pm z_d 2c/a_1^2\nu$.

   Therefore $A_2^2(z^*,\nu)$ can be approximated by

$$A_2^2(z^*,\nu)=\left|\frac{\sin N(\pm\pi\pm\xi)}{\sin(\pm\pi\pm\xi)}\right|^2\approx N^2e^{-\left(\frac{N\xi}{\sqrt{3}}\right)^2}=\tilde{A}_2^2$$

   with

$$\xi=\frac{\pi\nu a_1^2}{2c}\left(\frac{1}{z}-\frac{1}{z^*}\right)\approx\pi\left(\frac{\nu-\nu_0}{\nu_0}\right).$$

3) $A_1^2(z,\nu)$ at z^* is replaced by $A_1^2(z_1^*,\nu)$, z_1^* being the position of the maximum of the grating lobes for a wide-band signal. This maximum is obtained for the highest frequency of the transmitted signal which is considered to be $\nu_0+B/2$. Then $z_1^*=z_d/1+kz_d2c/a_1^2(\nu_0+B/2)$. This assumption has been validated with computer simulation within the frequency range generally used in HIFU. Hence, $A_1^2(z^*,\nu)\approx A_1^2(z_1^*,\nu_0)$ and $A_1^2(z_d,\nu)\approx A_1^2(z_d,\nu_0)$.

   Using these assumptions, (10) becomes

$$R=\frac{A_1^2(z_1^*,\nu_0)\int_{-\infty}^{+\infty}\tilde{A}_2^2\times B\times e^{-\left(\frac{\nu-\nu_0}{B}\right)^2}d\nu}{A_1^2(z_d,\nu_0)\int_{-\infty}^{+\infty}N^2\times B\times e^{-\left(\frac{\nu-\nu_0}{B}\right)^2}d\nu}$$

   and

$$R\approx\frac{R_0}{\sqrt{1+\left(\frac{\pi N}{\sqrt{3}}\times\frac{B}{\nu_0}\right)^2}}\times R_0^* \tag{12}$$

   where R_0 is the ratio defined by (11), $R_0^*=A_1^2(z_1^*,\nu_0)/A_1^2(z^*,\nu_0)$.

Although the ratio R_0^* depends on the bandwidth B, Fig. 2 shows that its variation as a function of B is negligible in comparison with that of the parameter $\sqrt{1+(\pi N/\sqrt{3}\times B/\nu_0)^2}$.

Equation (12) confirms a point already known, namely that the amplitude of the grating lobes decreases as the number of rings N increases. It also helps to understand through which parameter a wide-band signal reduces the amplitude of these lobes: the wider the bandwidth of the signal, the smaller the ratio R. It should be noted that for a zero bandwidth, we obtain the value of the ratio R for a single frequency signal, i.e., $R=R_0$.

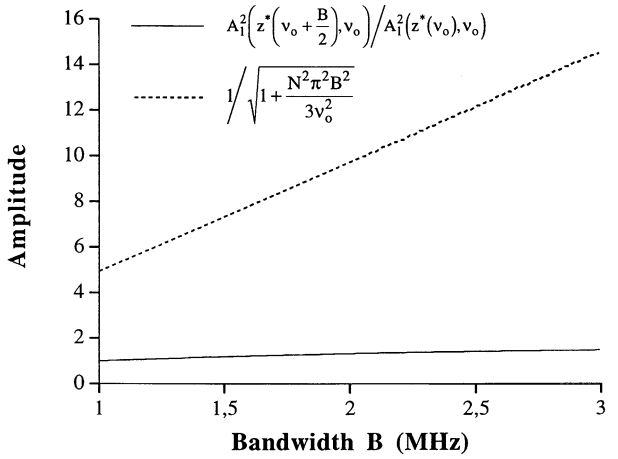

Fig. 2. Comparison between R_o^* and denominator of (12) as a function of the signal bandwidth (calculated with parameters of transducer $T1$).

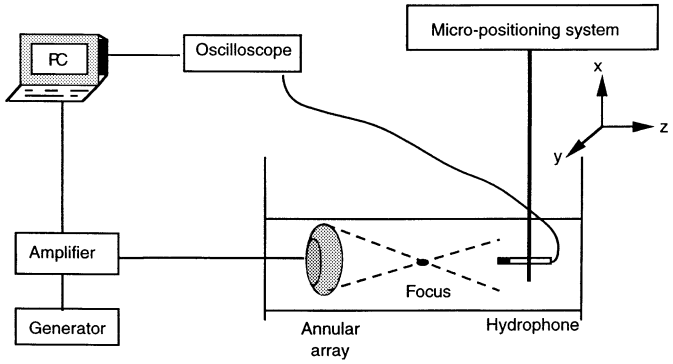

Fig. 3. Block diagram of the experimental system.

III. Materials and Methods

A. Choice of the Wide-Band Signal

A CW wide-band signal is characterized by a correlation function $C_{ss}(\tau)$ which displays a maximum at $\tau = 0$ and quickly tends toward zero when the delay τ increases. Pseudorandom phased modulated signals belong to this category and moreover they are easily generated with a mean power to peak power ratio close to unity. A type of pseudorandom code is known as a maximum length code ("m code"), based on an irreducible polynomial of order n. It is generated as a continuous burst of binary pulses each of length T, which gives the appearance of being random, but which in fact has a period of $T_s = (2^n - 1)T$. The correlation function of such a code can be shown to have an envelope in $\mathrm{sinc}^2(\pi\nu T)$ and a bandwidth of $B = 1/T$. The code modulates a carrier at the resonance frequency ν of the transducer in frequency or in phase in order to match the signal to the transducer bandwidth.

B. Experimental System

Two annular array transducers $(T1)$ and $(T2)$ (Imasonic, Besançon, France), whose characteristics are given in Table I, were used successively. Both transducers were made from a high-power piezocomposite material of class 1–3 with a $\lambda/4$ matching layer of 3.4 MRayl on the front face and an air-backed construction. It is well known that piezocomposite materials can be easily shaped and do not need to be physically cut out in elementary spherical transducers. Furthermore, they allow the construction of wide-band transducers with a simple design. All rings were electrically matched to 50 Ω with a transformer network.

The experimental verifications of the theoretical results were performed using the system shown in Fig. 3. The setup comprised a generator coupled to an eight-track power amplifier (INSERM U281, Lyon, France) supplying the transducer arrays. The generator provided either a single frequency signal at 2.25 MHz for $T1$ and 1.1 MHz for $T2$ or a modulated signal. The modulation involved either inverting or not inverting the phase of the single frequency signal at each period according to the state of the pseudorandom code. In this way, the bandwidth of the modulated signal was 50% of the signal frequency. Each channel of the amplifier could deliver a power of up to 40 W, but was set to 10 W in the experiments. The delays were calculated by a PC for each variable focus according to the geometry of these arrays. To obtain a resolution equivalent to one tenth of the signal period, each delay was coded on six bits.

In a tank filled with degassed and deionized water, a PVDF bilaminar shielded membrane hydrophone (Marconi Research, U.K.), with an active element of 0.5 mm, was displaced mechanically along the acoustic axis of the arrays $T1$ or $T2$, using an XYZ positioner (Microcontrole, Evry, France) with a resolution of 10 μm. The pressure signal received by the hydrophone was sampled using a digital oscilloscope (Tektronik 2430A, USA) and then transmitted to the computer for further processing and display of the results. The I_{SPTA} as defined in the theoretical approach had to be calculated over the whole length of the ultrasonic burst. In practice this was not possible because, on one hand, the memory of the oscilloscope was too small to digitize the signal corresponding to a burst of a few seconds, and on the other hand, the hydrophone would not have supported the energy. So the signal was transmitted with a 1% duty cycle compatible with the hydrophone capabilities. Several pressure readings were made for each position in order to reconstruct the whole transmitted signal. The intensity at one point was then obtained by integrating all the readings.

The theoretical approach was validated by comparing the obtained results of a known simulation method, i.e., the impulse response method [14] with different experimental results.

IV. Results and Discussion

Equations (4), (9), (10), and (12) were used for the computation of the theoretical I_{SPTA} and the theoretical ratio R.

Fig. 4 gives the I_{SPTA} as a function of the axial distance. For a single frequency signal, the measured data and simulated values using (4) are shown by dotted and solid lines, respectively. Fig. 4(a) and (b) corresponds, respectively, to the transducers $T1$ and $T2$ with variable foci positioned at 48

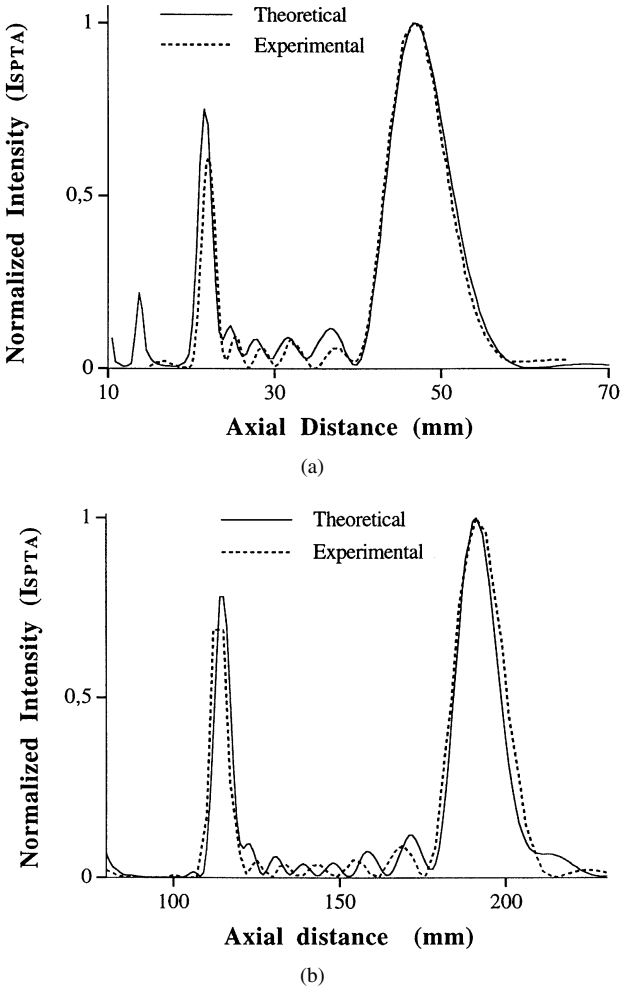

Fig. 4. On-axis I_{SPTA} obtained with a single frequency CW signal for both transducers described in Table I: (a) $T1$ with variable focus set at 48 mm, (b) $T2$ with variable focus set at 190 mm.

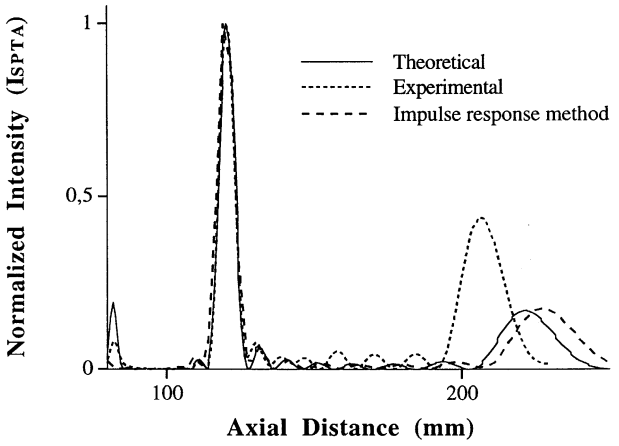

Fig. 5. On-axis I_{SPTA} of $T2$ with variable focus set at 120 mm obtained with a single frequency CW signal. Solid line represents intensity calculation from (9), dashed line is result of the impulse response method, and dotted line corresponds to experimental data.

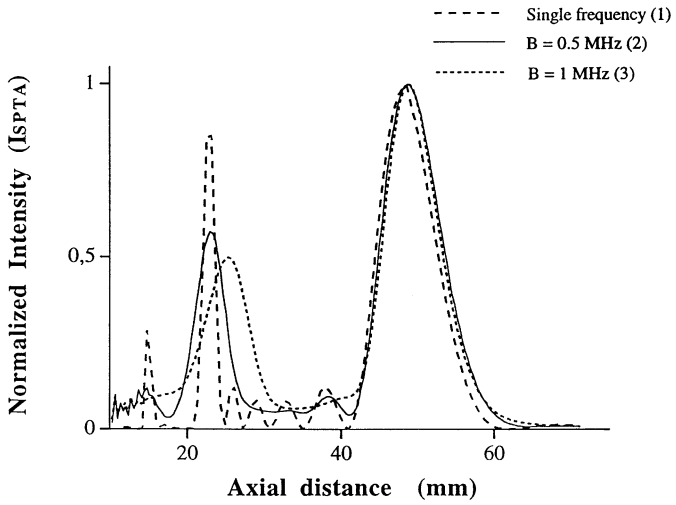

Fig. 6. On-axis I_{SPTA} of $T1$ with variable focus set at 48 mm, calculated from (9) for different values of the bandwidth B.

and 190 mm. As can be seen, there is a good correspondence between the measured and calculated curves.

According to (6), the positions of the grating lobes are calculated to be 21.29 mm for $T1$ and 109.38 mm for $T2$. Experimentally obtained, these two positions are 21.88 mm for $T1$ and 109.27 mm for $T2$. Fig. 5 presents the I_{SPTA} as a function of the axial distance for transducer $T2$ focused at 120 mm. The solid and dashed curves represent the I_{SPTA} intensity computed with (4) and with the impulse response method, respectively. The dotted curve gives the I_{SPTA} obtained experimentally. There is discrepancy between the experimental results and the theory when the aperture angles θ are larger than 30°. A focus at 120 mm for $T2$ corresponds to an aperture angle of 37°. This limitation exists whatever the size of the transducer. It is interesting to note that the impulse response method presents the same conditions of validity as the analysis presented in this work. One of the most useful advantages of (4) and (5) is the ability to obtain the undesirable focal zones very quickly and very accurately. From an experimental point of view, it is shown that the device developed for the generation of variable foci with an annular array works well with single frequency signals.

Fig. 6 shows the influence of the bandwidth of the phase modulated signal on the grating lobes, for the transducer $T1$ with a field focused at 48 mm. It gives the I_{SPTA} calculated from (9) as a function of the axial distance for different values of the bandwidth B of the coded signal. The dashed line (curve 1) represents the case of a single frequency CW signal ($B = 0$), the solid line (curve 2) corresponds to a bandwidth of 0.5 MHz, and the dotted line (curve 3) to a bandwidth of 1 MHz. As shown in the first part of the paper, the intensity of the grating lobes decreases significantly as the bandwidth of the signal widens. From the different results presented in this figure, it appears that the location of the grating lobes depends greatly on parameter B. This is easily observed by comparing curves 1 and 3. On curves 1 and 2, however, the location of the grating lobes is approximately the same. Based on the latest results, the location of the grating lobes can be considered as constant and equal to $z^*(\nu_0)$ for $B/\nu_0 < 0.2$. This condition is also valid for the transducer $T2$. In this case,

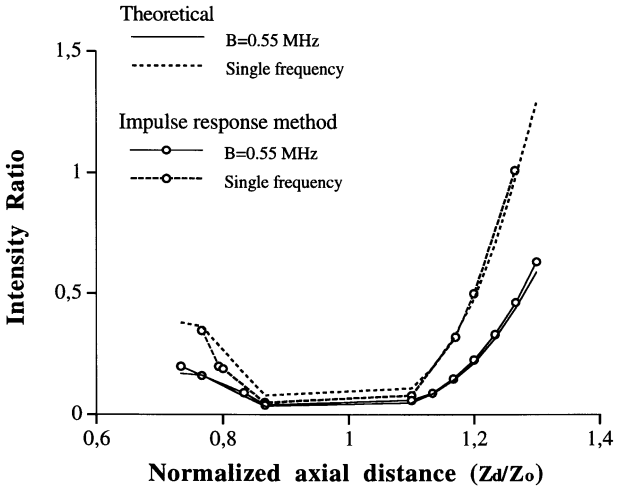

Fig. 7. Comparison of the ratio R of $T2$ given by (12) with the ratio R calculated by impulse response method versus the variable focus distance normalized to the geometric focus distance.

(12) is rewritten as

$$R \approx \frac{R_0}{\sqrt{1+\left(\frac{\pi N}{\sqrt{3}} \times \frac{B}{\nu_0}\right)^2}}.$$

Fig. 7 gives the ratio R as a function of the variable focus normalized to the geometric focal distance of the transducer (z_d/z_0). These results are given by simulating $T2$ with a bandwidth of 0.55 MHz. The open circle curves are obtained with the impulse response method using the same simulation parameters as for the developed theory with identical conditions. As can be observed, the two curves coincide, demonstrating once again the validity of the developed theory and the defined limitations are approximately well confirmed.

In practice, for a maximum reduction of the grating lobe amplitude, the bandwidth of the signal must be as large as possible, and so equals the bandwidth of the transducer.

Fig. 8 presents the experimental results of the measurements of the I_{SPTA} as a function of the axial distance for the transducers $T1$ and $T2$ and for a pseudorandom phase modulated signal with a bandwidth of 1.125 MHz and 0.55 MHz, respectively. As previously in Fig. 4, the transducers $T1$ and $T2$ have their variable foci at 48 and 190 mm, respectively. We observe that theory and experimentation are in good agreement. The comparison between Figs. 4 and 8 shows that the use of a wide-band signal enables us to reduce the grating lobes significantly. The results also show an axial widening of the grating lobes which is a direct consequence of the reduction of diffraction effects in transversal planes. Although the energy passing through the tissue is the same for both signals, the thermal effects should be lower with a wide-band signal, since it is known that for short exposure (<5 s), the temperature distribution follows the ultrasound beam pattern.

Ratio R for the transducer $T2$ is represented in Fig. 9, for different variable foci between 110 and 200 mm and in the case of a pseudorandom phase modulated signal (dotted line) and of a single frequency CW signal (solid line). The open

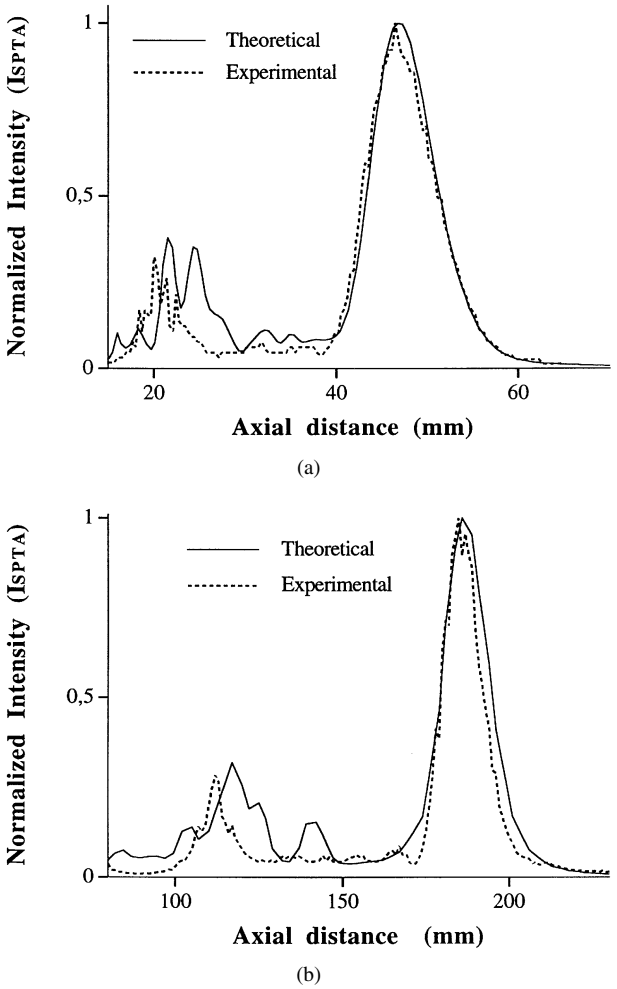

Fig. 8. Measured and calculated on-axis I_{SPTA} for a bandwidth B equal to the measured transducer bandwidth: (a) $T1$ with variable focus set at 48 mm, (b) $T2$ with variable focus set at 190 mm.

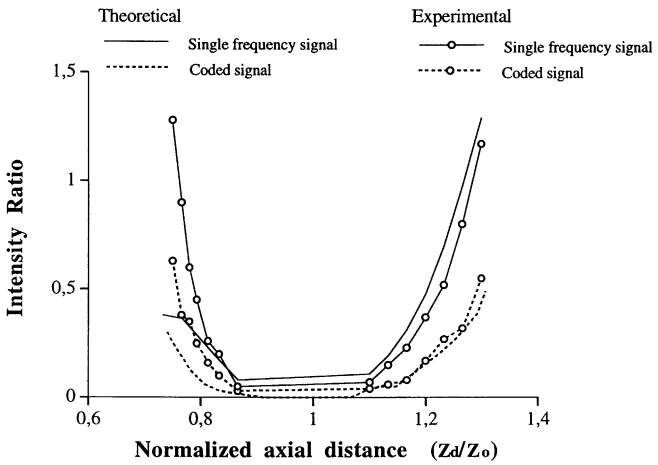

Fig. 9. Experimental and theoretical ratio R obtained with the transducer $T2$.

circle curves give the theoretical results for comparison. We should again note that the theory and the measurements differ as the variable focus moves closer to the transducer.

By comparing the experimental curves obtained, we observe that a wide-band CW signal permits a clear increase of the

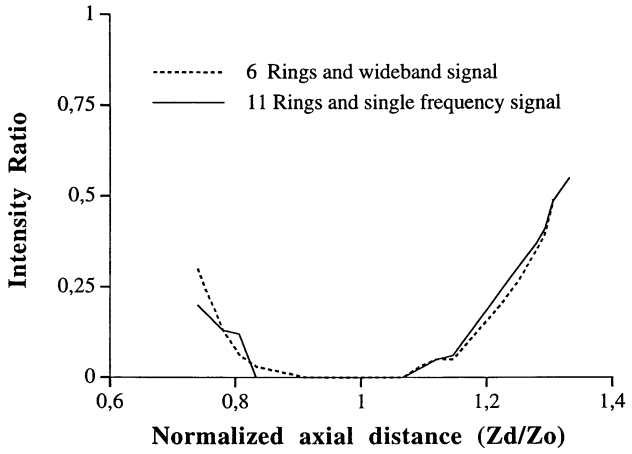

Fig. 10. Comparison of a six-ring annular array fed with a wide-band CW signal (dotted line) with an 11-ring annular array fed with a single frequency CW signal (solid line).

effective variable focus range in comparison with a single frequency CW signal. This zone rises for $T1$ from 18 to 27 mm, and for $T2$ from 60 to 82.5 mm. The use of a wide-band signal therefore enables us to increase the dynamic focusing range by nearly 50% for $T1$ and 30% for $T2$.

Fig. 10 presents two curves simulated for $T1$. One curve is obtained with a wide-band CW signal and six rings, the other curve is obtained with a single frequency signal and 11 rings. The use of a wide-band signal reduces the number of rings in the array by almost half.

In an annular array transducer, the interelement space must be large enough both to decrease electroacoustic couplings and to avoid the risk of an electrical breakdown when using high power ratings. So the number of rings cannot be increased indefinitely. A wide-band signal reduces the complexity of the electronic circuits and is therefore cheaper, but also helps to push back the boundaries of technology.

These experiments were performed in a nonattenuating medium. To keep the efficacy of the method in focused ultrasound surgery, it will be necessary to compensate the tissue attenuation which is a function of the frequency. However, this function is known at each depth of tissue, in particular at the location of the grating lobe. To compensate for this effect then, the solution is to prefilter the signal by the inverse function of the attenuation.

V. Conclusion

Considering ultrasound therapy as an application of the variable focus probe, a good alternative for minimizing the number of rings is to use a wide-band CW signal as, for example, a signal phase modulated by a pseudorandom code. Using an analytical expression, it has been shown that the intensity ratio between grating lobes and the main lobe was inversely proportional to the number of rings of the transducer and to the bandwidth of the transmitted signal. Using two different transducers, a series of experiments validated the use of a wide-band CW signal with the aim of increasing the dynamic focusing range, and so pushing back the technological boundaries usually encountered.

Moreover, it was observed during the experiments performed in this study that the use of a wide-band CW signal increases the cavitation threshold significantly. This discovery has been presented in a new paper [15].

The use of a wide-band CW signal should also enable the operator to optimize the adaptation of the focus range, to improve the control of the burst parameters, and to improve the control of the lesion for future applications of HIFU in ultrasound surgery.

References

[1] W. J. Fry, W. H. Mosberg, W. J. Barnard, and F. J. Fry, "Production of local destructive lesions in the central nervous system with ultrasound," *J. Neurosurgery*, no. 11, pp. 471–478, 1954.

[2] R. Bihrle, R. S. Foster, N. T. Sanghvi, J. P. Donohue, and P. J. Hood, "High intensity focused ultrasound for the treatment of benign prostatic hyperplasia: Early United States experience," *J. Urology*, vol. 151, pp. 1271–1275, 1994.

[3] S. Madersbacher, C. Kratzik, N. Szabo, M. Susani, L. Vingers, and M. Marberger, "Tissue ablation in benign prostatic hyperplasia with high intensity focused ultrasound," *J. Urology*, vol. 152, pp. 1956–1961, 1994.

[4] A. Gelet, J. Y. Chapelon, R. Bouvier, R. Souchon, C. Pangaud, A. F. Abdelrahim, D. Cathignol, and J. M. Dubernard, "Treatment of prostate cancer with transrectal focused ultrasound: Early clinical experience," *Eur. Urology*, vol. 29, pp. 174–183, 1996.

[5] J. Y. Chapelon, P. Faure, M. Plantier, D. Cathignol, R. Souchon, F. Gorry, and A. Gelet, "The feasibility of tissue ablation using high intensity electronically focused ultrasound," in *Proc. IEEE 1993 Ultrasonics Symp.*, pp. 1211–1214.

[6] E. S. Ebbini and C. A. Cain, "Experimental evaluation of a prototype cylindrical section ultrasound hyperthermia phased-array," *IEEE Trans. Ultrason., Ferroelect., Freq. Contr.*, vol. 38, pp. 510–520, Sept. 1991.

[7] S. I. Umemura and C. A. Cain, "The sector-vortex phased array: Acoustic field synthesis for hyperthermia," *IEEE Trans. Ultrason., Ferroelect., Freq. Contr.*, vol. 36, pp. 249–257, Mar. 1989.

[8] K. Hynynen, "The threshold for thermally significant cavitation in dog's thigh muscle in vivo," *Ultrasound Med. Biol.*, vol. 17, no. 2, pp. 157–169, 1991.

[9] E. Brookner, "Phased array radars," *Sci. Amer.*, vol. 252, no. 2, p. 94, 1985.

[10] J. Y. Chapelon, "Pseudo random correlation imaging and system characterization," in *Progress in Medical Imaging*, V. L. Newhouse Ed. New York: Springer-Verlag, 1988, pp. 227–246.

[11] A. Gelet, J. Y. Chapelon, J. Margonari, Y. Theillere, F. Gorry, D. Cathignol, and E. Blanc, "Prostatic tissue destruction by high intensity focused ultrasound: Experiments on canine prostate," *J. Endourology*, vol. 3, pp. 249–253, 1993.

[12] C. I. Zanelli, S. DeMarta, C. W. Hennige, and M. M. Kadri, "Beamforming for therapy with high intensity focused ultrasound (HIFU) using quantitative schlieren," in *Proc. 1993 IEEE Ultrasonics Symp.*, pp. 1233–1238.

[13] H. T. O'Neil, "Theory of focusing radiators," *J. Acoust. Soc. Amer.*, vol. 21, no. 5, pp. 516–526, Sept. 1949.

[14] M. Arditi, S. Foster, and W. J. Hunt, "Transient fields of concave annular arrays," *Ultrason. Imag.*, vol. 3, pp. 37–61, 1981.

[15] J. Y. Chapelon, F. Dupenloup, H. Cohen, and P. Lenz, "Reduction of cavitation using pseudo-random signals," *IEEE Trans. Ultrason., Ferroelect., Freq. Contr.*, vol. 43, pp. 623–625, July 1996.

Florence Dupenloup was born in Rilleux, France, on March 2, 1970. She received the M.S. degree in acoustics from the University of Lyon, France in 1993. She is presently a doctoral candidate at Unit 281 of the Institut National de la Santé et de la Recherche Médicale, Lyon, France.

Her research interests center on signal processing in ultrasound therapy.

Jean Yves Chapelon (M'89) was born in France on April 9, 1953. He received the M.S. degree from the University Jean Monet, Saint Etienne, France and the docteur-ès-sciences degree from the Lyon I University, Lyon, France in 1976 and 1988, respectively.

Since 1978, he has been with the Institut National de la Santé et de la Recherche Médicale where he is presently Director of Research. His current research interests in biomedical ultrasound include development of high-power ultrasound devices for therapy and interactions of ultrasound with tissue.

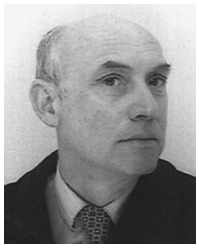

Dominique J. Cathignol (M'92) was born in Tours, France, on July 30, 1944. He received the diploma degree in electronic engineering and the docteur ingénieur and docteur es sciences degrees from the Institut National des Sciences Appliquées, Lyon, France in 1967, 1971, and 1980, respectively.

Since 1972, he has worked at the Institut National de la Santé et de la Recherche Médicale, Lyon, France. Since 1987, he has been the Director of Research Unit of a biomedical engineering unit entitled "Applications Médicales des Ultrasons et des Rayonnements Non Ionisants." The research topic of the laboratory concerns noninvasive techniques for diagnosis and therapy using Doppler effect, shock waves, high ultrasonic energy, high ultrasonic frequency, bio-impedance, and phototherapy.

Oleg A. Sapozhnikov was born in Batyrevo, Russia, on July 28, 1962. He received the M.S. degree in physics and the Ph.D. degree in acoustics from M. V. Lomonosov Moscow State University (MSU) in 1985 and 1988, respectively.

Since 1988 he has been with Department of Acoustics, Physics Faculty, MSU, where now he is an Associate Professor. During 1994 he worked in Unit 281 of the Institut National de la Santé et de la Recherche Médicale, Lyon, France, as a Foreign Researcher. His main activities are the fields of nonlinear acoustics, optoacoustics, and the general theory of waves.